

# Current and future burden of Ross River virus infection attributable to increasing temperature in Australia: a population-based study



Yohannes Tefera Damtew,<sup>a,b</sup> Blesson Mathew Varghese,<sup>a</sup> Olga Anikeeva,<sup>a</sup> Michael Tong,<sup>c</sup> Alana Hansen,<sup>a</sup> Keith Dear,<sup>a</sup> Ying Zhang,<sup>d</sup> Geoffrey Morgan,<sup>d</sup> Tim Driscoll,<sup>d</sup> Tony Capon,<sup>e</sup> Michelle Gourley,<sup>f</sup> Vanessa Prescott,<sup>f</sup> and Peng Bi<sup>a,\*</sup>



<sup>a</sup>School of Public Health, The University of Adelaide, Adelaide, South Australia, 5005, Australia

<sup>b</sup>College of Health and Medical Sciences, Haramaya University, P.O.BOX 138, Dire Dawa, Ethiopia

<sup>c</sup>National Centre for Epidemiology and Population Health, ANU College of Health and Medicine, The Australian National University, Canberra, ACT 2601, Australia

<sup>d</sup>School of Public Health, Faculty of Medicine and Health, The University of Sydney, New South Wales, 2006, Australia

<sup>e</sup>Monash Sustainable Development Institute, Monash University, Melbourne, Victoria, Australia

<sup>f</sup>Burden of Disease and Mortality Unit, Australian Institute of Health and Welfare, Canberra, ACT 2601, Australia

## Summary

**Background** Ross River virus (RRV), Australia's most notifiable vector-borne disease transmitted through mosquito bites, has seen increased transmission due to rising temperatures. Quantifying the burden of RRV infection attributable to increasing temperatures (both current and future) is pivotal to inform prevention strategies in the context of climate change.

**Methods** As RRV-related deaths are rare in Australia, we utilised years lived with disability (YLDs) associated with RRV infection data from the Australian Institute of Health and Welfare (AIHW) Burden of Disease database between 2003 and 2018. We obtained relative risks per 1 °C temperature increase in RRV infection from a previous meta-analysis. Exposure distributions for each Köppen-Geiger climate zone were calculated separately and compared with the theoretical-minimum-risk exposure distribution to calculate RRV burden attributable to increasing temperatures during the baseline period (2003–2018), and projected future burdens for the 2030s and 2050s under two greenhouse gas emission scenarios (Representative Concentration Pathways, RCP 4.5 and RCP 8.5), two adaptation scenarios, and different population growth series.

**Findings** During the baseline period (2003–2018), increasing mean temperatures contributed to 35.8 (±0.5) YLDs (19.1%) of the observed RRV burden in Australia. The mean temperature attributable RRV burden varied across climate zones and jurisdictions. Under both RCP scenarios, the projected RRV burden is estimated to increase in the future despite adaptation scenarios. By the 2050s, without adaptation, the RRV burden could reach 45.8 YLDs under RCP4.5 and 51.1 YLDs under RCP8.5. Implementing a 10% adaptation strategy could reduce RRV burden to 41.8 and 46.4 YLDs, respectively.

**Interpretation** These findings provide scientific evidence for informing policy decisions and guiding resource allocation for mitigating the future RRV burden. The current findings underscore the need to develop location-specific adaptation strategies for climate-sensitive disease control and prevention.

**Funding** Australian Research Council Discovery Program.

**Copyright** © 2024 The Authors. Published by Elsevier Ltd. This is an open access article under the CC BY-NC-ND license (<http://creativecommons.org/licenses/by-nc-nd/4.0/>).

**Keywords:** Ross River virus; Burden of disease; Climate change; Attributable burden; Adaptation

The Lancet Regional Health - Western Pacific 2024;48: 101124

Published Online xxx  
<https://doi.org/10.1016/j.lanwpc.2024.101124>

\*Corresponding author. School of Public Health, The University of Adelaide, Adelaide, SA, 5005, Australia.

E-mail addresses: [peng.bi@adelaide.edu.au](mailto:peng.bi@adelaide.edu.au) (P. Bi), [yohannestefera.damtew@adelaide.edu.au](mailto:yohannestefera.damtew@adelaide.edu.au) (Y.T. Damtew), [blesson.varghese@adelaide.edu.au](mailto:blesson.varghese@adelaide.edu.au) (B.M. Varghese), [olga.anikeeva@adelaide.edu.au](mailto:olga.anikeeva@adelaide.edu.au) (O. Anikeeva), [Michael.Tong@anu.edu.au](mailto:Michael.Tong@anu.edu.au) (M. Tong), [alana.hansen@adelaide.edu.au](mailto:alana.hansen@adelaide.edu.au) (A. Hansen), [keith.dear@adelaide.edu.au](mailto:keith.dear@adelaide.edu.au) (K. Dear), [ying.zhang@sydney.edu.au](mailto:ying.zhang@sydney.edu.au) (Y. Zhang), [geoffrey.morgan@sydney.edu.au](mailto:geoffrey.morgan@sydney.edu.au) (G. Morgan), [tim.driscoll@sydney.edu.au](mailto:tim.driscoll@sydney.edu.au) (T. Driscoll), [tony.capon@monash.edu](mailto:tony.capon@monash.edu) (T. Capon), [michelle.gourley@aihw.gov.au](mailto:michelle.gourley@aihw.gov.au) (M. Gourley), [vanessa.prescott@aihw.gov.au](mailto:vanessa.prescott@aihw.gov.au) (V. Prescott).

### Research in context

#### Evidence before this study

Epidemiological studies have shown that temperature plays a crucial role in the transmission of Ross River Virus infection (RRV), the most notified vector-borne disease in Australia, Western Pacific Region. However, these studies have mainly focused on disease incidence and have not provided evidence on the years of life lost (YLL) and years lived with disability (YLD) caused by RRV infection, nor future burden projections through our comprehensive literature search.

#### Added value of this study

To the best of our knowledge, this is the first international study to quantify the current and future burden of RRV attributed to increasing temperature at national level, using Global Burden of Disease approach. We estimated the burden of RRV attributed to increasing temperature across different climate zones and jurisdictions in Australia, considering future population changes and adaptation scenarios. Our findings revealed substantial geographical variations, with the highest burden observed in tropical climates. Additionally, our results demonstrated that rising temperatures increased the burden of RRV infection, with varying impacts depending on the

climate zone and jurisdiction in Australia. Furthermore, the magnitude of this change depends on the demographic and climate change scenarios. Notably, the change in population size and adaptation scenarios led to a significant variation in the temperature-attributable burden, as compared to the differences resulting from changes in emission scenarios.

#### Implications of all the available evidence

Our study shows the impact of increasing temperatures on the burden of RRV in various climate zones and jurisdictions across Australia. Such findings will enhance our understanding of how rising temperatures contribute to the burden of RRV and facilitate the development of public health policies to address the challenges posed by climate change. Additionally, this study not only examines the variations in RRV burden associated with temperature across different climatic zones but also analyses the influence of adaptation scenarios and changes in population size. These findings will provide crucial evidence in climate change mitigation and adaptation policies and assist in formulating regional and location-specific adaptation strategies to reduce the burden of RRV in the context of climate change.

## Introduction

Climate change poses a significant threat to human health, including through the amplification of vector-borne diseases.<sup>1,2</sup> Ongoing climate change is causing global shifts in temperature and precipitation patterns, profoundly impacting the incidence, severity and duration of these diseases.<sup>3-9</sup> The relationship between temperature and transmission of vector-borne diseases has been an increasing public health concern.<sup>8-10</sup> One such vector-borne disease that exemplifies the interplay between climatic factors and disease transmission is Ross River virus (RRV) infection, the most prevalent mosquito-borne disease in Australia.<sup>7</sup>

RRV is transmitted to humans primarily through bites of an infected mosquito and, while rarely fatal, can result in long-term disability, impacting quality of life for those affected.<sup>11,12</sup> The incidence of RRV infection is sensitive to fluctuations in climatic factors such as temperature, rainfall and relative humidity.<sup>5,13</sup>

Epidemiological studies have demonstrated that temperature is an important environmental determinant in the transmission of RRV.<sup>14-16</sup> Multiple studies revealed that global warming can increase the transmission and risk of RRV infection.<sup>7,17,18</sup> Understanding how temperature variations, especially in the context of climate change, influence the burden of RRV infection is important for public health preparedness and response.<sup>5,7</sup> However, most studies have focused on disease incidence, overlooking years of life lost (YLL) and years lived with disability (YLD) related to RRV infection. Quantifying the disease burden attributed to

increasing temperature is pivotal for informing prevention strategies and assessing health-related losses.<sup>19,20</sup>

While there is substantial evidence pointing to direct influence of climatic patterns (including fluctuations in temperature and rainfall) on the transmission of vector-borne diseases, uncertainties persist in reliably forecasting the future impact of climate change on these diseases.<sup>21</sup> Therefore, we explore the temperature-attributable burden of RRV infection, using health indicators consistent with the Global Burden of Disease study.<sup>22,23</sup> The research highlights geographical disparities by estimating the burden of disease across multiple climate zones and jurisdictions. Additionally, the study projects the potential future impact of increasing temperature on the burden of RRV under different climate, demographic and adaptation scenarios for the 2030s and 2050s in Australia.

## Methods

### Burden of disease data

Data on the annual burden of RRV infection were obtained from the Australian Institute of Health and Welfare (AIHW), an official national health outcome data custodian in Australia.<sup>12</sup> Given the rarity of deaths related to RRV infection in Australia, our analysis focused solely on years lived with disability (YLDs). YLDs represent the amount of time equivalent to one full year of healthy life that is lost due to disability or ill health.<sup>22,23</sup> The AIHW provided estimates of national-level YLD estimates for the years 2003, 2011, 2015 and

2018. State and Territory level estimates were available for those years (except 2003 due to data availability). For the intervening years between 2003 and 2018, state and territory YLDs were obtained using linear interpolation approach, and the annual average YLDs were then calculated for the baseline period (2003–2018). We further disaggregated the YLD at State/Territory level to climate zones level using the proportion of RRV cases and population distribution in each climate zone and jurisdiction (State and Territory), assuming the number of cases is proportional to the number of YLD (Table S1). The total numbers of RRV cases for the baseline period (2003–2018) in each climate zone and jurisdiction were sourced from the Australian National Notifiable Diseases Surveillance System (NNDSS) public datasets and Department of Health and aged care.<sup>24</sup>

### Historical and future temperature data

Historical and future daily gridded minimum and maximum temperature data were obtained from Queensland Government's Long Paddock website which hosts the Scientific Information for Land Owners interpolated climate datasets.<sup>25</sup> The data presented as a raster dataset in NetCDF (network Common Data Form) format with a spatial resolution of 5 km by 5 km.<sup>26</sup> The raster data was spatially overlaid on top of the Australian Bureau of Statistics (ABS) Statistical Area Level 2 (SA2), which represents medium-sized general-purpose areas where communities interact socially and economically.<sup>27</sup> This overlay included Köppen-Geiger climate zone maps of Australia to acquire temperature data at the climate zone level.

Temperature projections based on Representative Concentration Pathways (RCPs), which are greenhouse gas concentration trajectories adopted by the IPCC, were used.<sup>28</sup> Specifically, RCP 4.5 and RCP 8.5, representing the intermediate/medium and high greenhouse gases emission scenarios, were selected for this study.<sup>28,29</sup> Projected temperatures for the periods 2016 to 2045 centred on the 2030s, and 2046 to 2065 centred on the 2050s, were obtained from 5 km daily gridded "application ready" data available using eight global scale climate models (GCMs) including Access 1.0, CESM1-CAM5, CNRM-CM5, GFDL-ESM2M, HadGEM2-CC, CanESM2, MIROC5, NorESM1-M). Each climate projection model included daily maximum and minimum temperatures, and the mean value was calculated from each model. To account for variability among different GCMs, we averaged the mean temperatures across all eight GCMs.<sup>30,31</sup>

### Population data

Population data were acquired from the ABS.<sup>32</sup> The baseline population for 2003–2018 was retrieved at SA2 level and summed to obtain the population in each State/Territory and climate zone. The future population projection based on low, medium and high growth

series for each State and Territory was also acquired from the ABS.<sup>33</sup> We divided the future projected population by the baseline population for each State/Territory to obtain the population growth factor. Subsequently, this factor was applied to estimate the future population size in specific climate zones within each State/Territory.

### Temperature-RRV infection relationships

Identifying the association of a disease with increased prevalence of exposure is the initial step in estimating attributable burden of a disease to a certain risk factor.<sup>19</sup> The association between temperature and incidence of RRV infection has been explored in several studies.<sup>14,15,34–37</sup> For this study, we used an established association from our previously published meta-analysis.<sup>17</sup> Briefly, the relative risks (RRs) from published studies were standardized per 1 °C change in temperature and a log-linear exposure–response function was derived from these studies using random-effect meta-analysis to describe the association between temperature and RRV infection.<sup>17</sup> Given the likely modifying effect of other climatic factors, we included only those studies that accounted for potential covariates including humidity and rainfall. In the meta-analysis, the RRs of RRV infection per 1 °C increase in temperature were analysed based on 12 Köppen-Geiger climate zones in Australia. This approach yielded effect estimates for five climate zones including Humid subtropical climate, Cold semi-arid climate, Oceanic climate, Warm summer Mediterranean climate and Tropical savanna climate. For the remaining climate zones ( $n = 7$ ), we used RRs from adjacent climate zones with a similar annual temperature as a proxy indicator for the risk of RRV infection associated with non-optimal temperatures due to limited published studies in these zones.

### Data analysis

#### *Population attributable fraction and disease burden*

The comparative risk assessment (CRA) framework, which uses a counterfactual risk exposure, was applied considering temperature as a monotonically increasing risk factor with a baseline threshold or theoretical minimum risk exposure distribution (TMRED).<sup>38</sup> For this study, the TMRED is the temperature at which the RR would be the lowest in an exposure-response curve or the exposure distribution that minimizes risk for the population. The mean annual temperature of each climate zone was assumed to be the TMRED. As studies included in the systematic review and meta-analysis used different threshold values and temperature metrics (minimum, maximum and mean temperature), we chose the mean temperature as a representative metric for this analysis. The daily mean temperatures for the baseline period (2003–2018) and projected years (2030s and 2050s) were arranged in increasing order and frequencies were calculated using a class width of 1 °C.

The prevalence of increasing mean temperature exposure to the risk factor was calculated for each climate zone as a proportion of days within a year having a temperature value above the TMRED.<sup>19</sup>

After determining the TMRED, the population attributable fraction (PAF) was calculated by assuming a log-linear function to calculate the change in RRs above TMRED.<sup>19</sup> The choice of the log-linear function was based on the observed relationship among included studies in the meta-analysis.<sup>17</sup>

Considering different climate zones, exposure categories (*c*), RR specific to the climate zone, and the prevalence of exposure to a risk factor in each climate zone (*P*), the PAF is calculated by the following generalized form<sup>39,40</sup>:

$$PAF = \frac{\sum_c cPc (RR - 1)}{\sum_c cPc (RR - 1) + 1} \times 100 \dots \dots \dots \text{equation (1)}$$

where,

$\sum_c$  is the sum of the proportion of the year above the TMRED for each categorised value of temperature in the distribution and the corresponding calculated RR (from the log linear function) for climate zones.

$RR = \exp(\beta\Delta T)$ ; where RR is the calculated relative risk of RRV infection above TMRED,  $\Delta T$  is the change in temperature above TMRED and  $\beta$  is the natural log of the relative risk at TMRED. The parameter  $\beta$  represents log (RR) of RRV risks associated with temperature exposure and obtained from the meta-analysis.

The attributable disease burden for the baseline period, 2030s and 2050s was estimated by multiplying the PAF by the corresponding YLDs. The climate zone-specific future temperature-attributable YLDs under different temperature and population projections were calculated as follows:

$$YLD_{temp} = p * \sum (PAF_i * YLD_i) \dots \dots \dots \text{equation (2)}$$

where  $YLD_{temp}$ ,  $PAF_i$  and  $YLD_i$  were temperature-attributable YLDs, PAFs and weighted YLDs at each climate zone level, respectively and *p* represents the population growth rate.

The state, territory and national attributable burdens of RRV infection due to increasing mean temperature were calculated by summing the subsets of temperature attributable burden from each climate zone. Finally, to facilitate a meaningful comparison of RRV burden attributable to temperature across climate zones and jurisdictions in Australia, we applied a population-standardized YLD rate per million population.

**Modelling adaptation**

Considering ongoing possible intervention or socio-economic adaptations in RRV infection control possible

adaptations scenarios are considered in this study.<sup>7,41,42</sup> Although there are several approaches in modelling adaptation scenarios, we chose the exposure–response function (ERF) slope reduction approach due to its empirical evidence base.<sup>41,42</sup> The adaptation scenario was developed based on exposure–response function (ERF) slope reduction using the change in relative risk across decades among studies included in the meta-analysis. We divided the studies based on study period into three decades and pooled the RR using random effect meta-analysis for each decade. By pooling RRs across each decade to obtain a single estimate per decade, our analysis showed a 5.9% reduction in the slope from the first to the last decade.<sup>42</sup> Based on this evidence and considering the confidence interval associated with this estimate, we applied a 5% and 10% slope reduction in ERF across all climate zones to account for adaptation as scenario analysis, and subsequently calculated the future PAF as mentioned earlier.

**Sensitivity analysis**

We ran several sensitivity analyses to test whether the results were robust to changes in the exposure or response of temperature-RRV curve. Temperature metrics, including the median of the mean temperature, the most frequent temperatures (MFT) and the mean temperature range of 17–32 °C, were used as TMREDS. The choice of 17–32 °C aligns with the temperature range favourable for mosquito-vectors in RRV transmission, as described in previous studies.<sup>13</sup> In addition, we assumed a future non-linear exposure-response and applied log-quadratic and log-cubic functions to calculate the RR above TMRED. Furthermore, we also considered the low and high population projection series. All analyses were performed using Microsoft Excel and the Python 2 programming language.<sup>19,43</sup>

**Role of the funding source**

The funder of the study had no role in study design, data collection, data analysis, data interpretation, or writing of the report.

**Results**

**Descriptive analysis**

Table 1 presents statistics on the baseline associations between temperature and RRV infection, the number of RRV infection cases, YLDs related to RRV infection, and temperature data. The average annual mean temperature varies across climate zones in Australia, ranging from 14.2 ± 4.3 °C in regions with an Oceanic climate (Cfb) to 26.1 ± 2.3 °C in areas with a Tropical savanna climate (Aw) (Figure S1). From 2003 to 2018, a total of 77,949 cases of RRV infection were reported, resulting in an annual average of 187.7 ± 33.7 YLDs per year. The highest rate of RRV cases (2626 cases per 100,000 population) and burden (80.3 YLDs per million) were

Climate zones	RR (95% CI) <sup>17</sup>	Number of cases	Mean YLD(SD) <sup>a</sup>	TMREds			
				Mean (SD) °C	Median °C	MFT °C	17–32 °C <sup>b</sup>
Af (Tropical rainforest)	1.24 (1.18–1.30) <sup>c</sup>	589	1.8 (0.4)	23.2 (2.6)	23.4	25.4	18.4
Am (Tropical monsoon)	1.24 (1.18–1.30) <sup>c</sup>	1894	5.8 (1.2)	24.7 (2.4)	24.9	27.1	20.1
Aw (Tropical savanna)	1.24 (1.18–1.30)	8585	23.3 (5.1)	26.1 (2.3)	27.0	27.7	21.7
BSk (Semi-Arid, cold desert)	1.02 (0.77–1.35)	6303	16.3 (0.3)	16.4 (4.9)	16.5	9.9	17.0
BSh (Semi-Arid, hot desert)	1.02 (0.77–1.35) <sup>d</sup>	4679	11.2 (0.9)	22.1 (4.9)	22.9	27.2	17.0
BWh (Arid, hot desert)	1.02 (0.77–1.35) <sup>d</sup>	2045	2.7 (1.6)	22.2 (5.5)	23.0	28.2	17.0
BWk (Arid, cold desert)	1.02 (0.77–1.35) <sup>d</sup>	1346	3.8 (0.5)	17.6 (5.5)	17.5	10.2	17.0
Cfa (Humid subtropical, hot summer)	1.11 (1.03–1.19)	34,617	94.8 (2.2)	19.3 (3.9)	19.7	13.2	17.0
Cfb (Oceanic, warm summer)	1.11 (1.03–1.19) <sup>e</sup>	4051	11.7 (3.4)	14.2 (4.3)	14.2	10.3	17.0
Cwa (Humid subtropical dry-winter)	1.11 (1.03–1.19) <sup>e</sup>	1277	3.9 (0.7)	22.7 (3.4)	23.4	7.8	17.0
Csb (Mediterranean, warm summer)	1.08 (1.05–1.11)	2750	4.6 (0.5)	15.6 (3.9)	15.3	22.8	17.0
Csa (Mediterranean hot summer)	1.08 (1.05–1.11) <sup>f</sup>	9813	7.8 (0.9)	18.5 (4.3)	18.2	25.8	17.0

RR, Relative risk; CI, Confidence interval; SD, Standard deviation; MFT, Most frequent temperature. <sup>a</sup>The mean YLD is the annual average across baseline period (2003–2018) for each jurisdiction. <sup>b</sup>The observed lowest value in the range 17–32 °C. <sup>c</sup>Aw relative risk used as proxy. <sup>d</sup>BSk relative risk used as proxy. <sup>e</sup>Cfa relative risk used as proxy. <sup>f</sup>Csb relative risk used as proxy.

**Table 1: Relative Risks (RR) per 1 °C increase in temperature, RRV infection cases, mean annual YLD and theoretical minimum risk exposure distribution (TMREds) by Köppen-Geiger climate zone in Australia, 2003–2018.**

observed in the Af climate zone, while the lowest rate (67 cases per 100,000) and burden (1.9 YLDs per million) were recorded in the Cfb climate zone (Table S2). At the jurisdiction level, the Northern Territory (NT) had the highest burden, with 41.7 YLDs per million, followed by Queensland (QLD) with 25.7 YLDs per million. Notably, despite the occurrence of RRV cases, YLDs related to RRV infection were non-existent in the Australian Capital Territory (ACT) and Tasmania (TAS) (Table 2).

### Temperature-RRV infection association

As shown in Table 1, there was an increase in the risk of RRV infection associated with a rise in temperature across all climate zones, although the association had a wider confidence interval in BWh, BWk, BSh, BSk climate zones. The largest significant association was

observed in tropical climate zones including Aw, Am, and Af with an RR of 1.24 (95% CI: 1.18–1.30).

### Population attributable fraction and temperature attributable burden of RRV infection

We estimated the PAF and YLDs attributable to increasing mean temperature in different climate zones and jurisdictions (Fig. 1 and Table 2). The PAF of RRV infection associated with increasing mean temperature varied considerably across climate zones. Tropical climate zones including Am, Aw and Af had the highest PAF with 28.8%, 28.0% and 24.4%, respectively (Table S2).

Nationally, 35.8 (±0.5) YLDs equivalent to 1.6 YLDs per million population were attributed to increasing mean temperature in Australia. This accounted for

State and territory	Population	YLDs (rate per million)	% of national YLDs	Temperature attributable YLDs		
				YLDs (SD)	% of state YLDs	YLDs per million population
NSW	7,203,978	23.5 (3.3)	12.5	4.1 (0.2)	17.4 (0.7)	0.57 (0.1)
VIC	5,554,022	22.7 (2.1)	12.1	3.2 (0.2)	14.1 (0.7)	0.58 (0.1)
QLD	4,408,955	113.1 (5.7)	60.3	23.7 (0.8)	21.0 (1.0)	5.40 (1.2)
WA	2,305,735	10.1 (1.4)	5.4	1.5 (0.1)	14.9 (0.8)	0.65 (0.2)
SA	1,630,083	8.8 (1.4)	4.7	0.8 (0.1)	9.1 (0.8)	0.50 (0.1)
TAS	505,773	0.0 (0.0)	0.0	0.0 (0.0)	0.0 (0.0)	0.0 (0.0)
NT	227,968	9.5 (1.7)	5.1	2.5 (0.2)	26.3 (1.0)	10.9 (1.4)
ACT	368,306	0.0 (0.0)	0.0	0.0 (0.0)	0.0 (0.0)	0.0 (0.0)
<b>National</b>	<b>22,204,820</b>	<b>187.7 (1.5)</b>	<b>100</b>	<b>35.8 (0.5)</b>	<b>-</b>	<b>1.6 (0.4)</b>

YLDs: Years lived with disability; NSW: New South Wales; VIC: Victoria; QLD: Queensland; WA: Western Australia; SA: South Australia; TAS: Tasmania; NT: Northern Territory; ACT: Australian Capital Territory.

**Table 2: Temperature-attributable YLD due to RRV infection by state and territory in Australia, 2003–2018.**

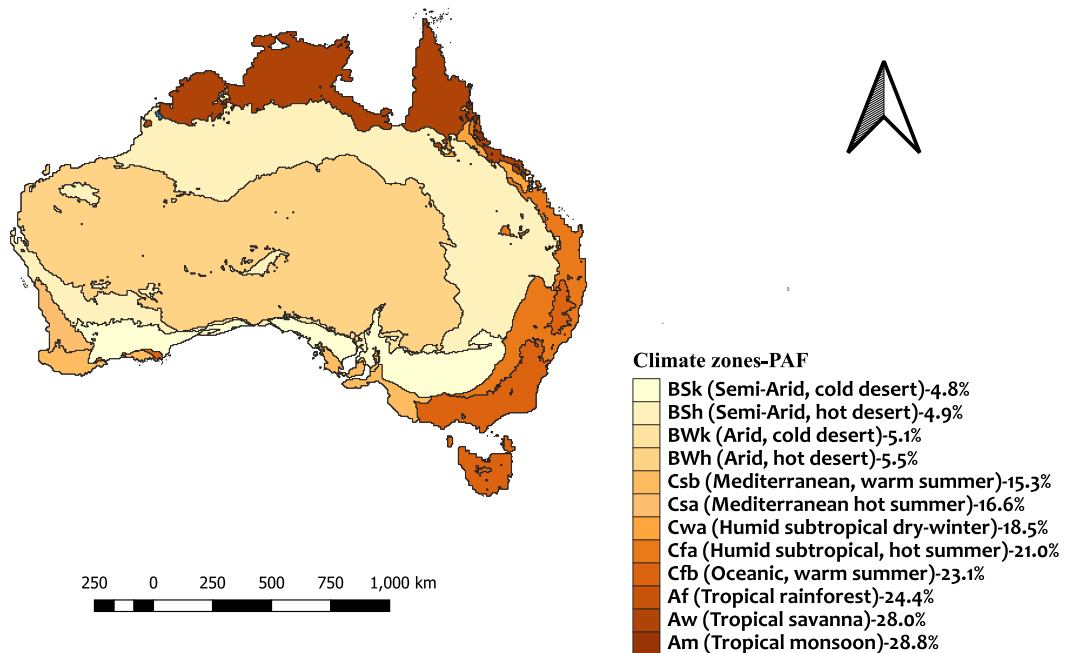


**Fig. 1:** Distribution of estimated population attributable fraction related to RRV infection by Koppen-Geiger climate zones in Australia across the baseline period 2003–2018.

19.1% of the total YLDs related to RRV infection being attributable to increasing mean temperature. At climate zone level, the highest and the lowest YLDs attributable burden to increasing mean temperature per million individuals was observed in Af (19.9 YLDs per million) and BSk (0.4 YLDs per million) climate zones, respectively (Table S2).

Further analysis at the jurisdiction level revealed that Queensland (QLD) had the highest proportion of temperature-attributable burden, accounting for 23.8 YLDs, which is 21% of the total YLD in the state (Table 2). Excluding ACT and Tasmania, where the YLD was nil, South Australia (SA) had the lowest proportion of temperature-attributable YLDs, with 0.8 YLDs, which is 9.1% of the SA total YLD. When considering the population size of each state, the attributable burden per million population ranged from 0.5 to 10.9 YLDs across states and territories. The temperature-attributable burden per million population at the state and territory levels was below the national average in all states except the Northern Territory (NT) and QLD. In NT and QLD, the burden was approximately seven and three times as high, respectively, as the national average YLDs per million population (Table 2).

Fig. 2 depicts the percentage distribution of YLDs per million population based on climate zone across states and territories. It is evident that the Aw climate zone accounted for the highest proportion of YLDs per million population in the Northern Territory (NT) and

Western Australia (WA), with percentages of 94.1% and 64.2% respectively. Conversely, in QLD, more than one-third of the temperature-attributable burden was linked to the Af climate zone. Additionally, the BWk, Cfa, and BSh climate zones in SA, VIC, and NSW respectively registered the highest temperature-attributable YLDs per million population.

#### Projected temperature and future attributable YLDs under population change and adaptation scenarios

Compared to the baseline period, the mean annual temperature is projected to increase under both RCP 4.5 and RCP 8.5 scenarios in the 2030s and 2050s, with distinct differences in the extent of temperature change across climate zones. In the 2030s, the highest mean annual temperature was observed in the Aw climate zone, with an average of  $27.1\text{ }^{\circ}\text{C} \pm 2.3$  under RCP 4.5 and  $27.3\text{ }^{\circ}\text{C} \pm 2.3$  under RCP 8.5. Similarly, for the 2050s, the projected mean annual temperature for the Aw climate zone was  $27.4\text{ }^{\circ}\text{C} \pm 2.3$  under RCP 4.5 and  $27.8\text{ }^{\circ}\text{C} \pm 2.3$  under RCP 8.5. In the other climate zones, the projected average annual mean temperature anomaly ranges from  $0.9\text{ }^{\circ}\text{C}$  to  $2.3\text{ }^{\circ}\text{C}$  under RCP 4.5 and  $1.3\text{ }^{\circ}\text{C}$ – $2.8\text{ }^{\circ}\text{C}$  under RCP 8.5 in the 2050s, compared to the baseline period (Supplementary Material, Table S1).

The PAF for each climate zone under selected RCPs (RCP4.5 and RCP8.5) and adaptation scenarios (5% and 10% slope reduction in ERF) is presented in the

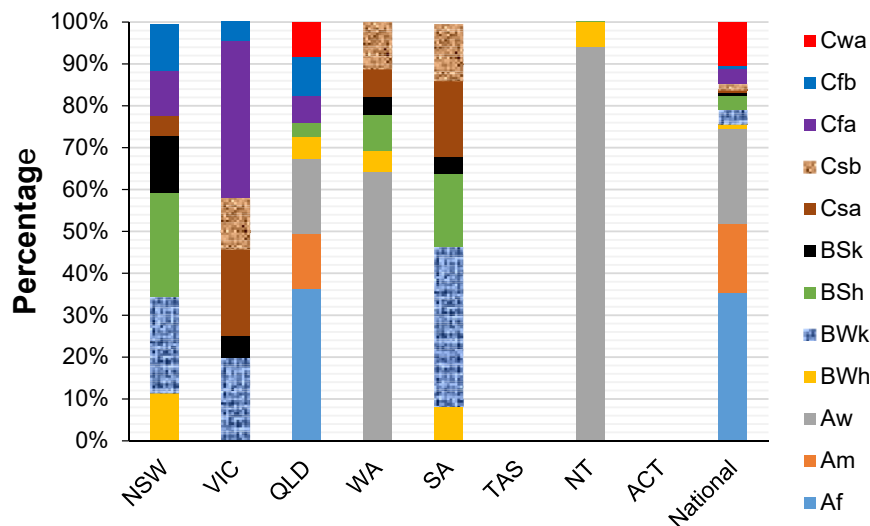


Fig. 2: Percentage distribution of YLDs per million population by climate zones in Australia and across states and territories during the baseline period, 2003–2018.

Supplementary Material (Figures S2 and S3). Despite applying adaptation scenarios, a gradual increase in PAFs was observed across climate zones in future periods with the rise in temperature.

Table 3 presents the overall projected mean temperature-attributable YLDs under two population and two adaptation scenarios. The details for each jurisdiction are presented in the Supplementary Material (Table S3). Fig. 3 shows projected YLDs per million population and the percentage change compared to the baseline period across different climate zones. Assuming a constant exposure-response function and TMRED, if the baseline population of Australia is exposed to the projected change in temperature by the

2050s under RCP 4.5 and RCP 8.5, the mean temperature-attributable YLDs would increase by 29.3% (from 35.8 YLDs to 45.8 YLDs) and by 46.6% (from 35.8 YLDs to 51.1 YLDs), respectively. In the same period and under both RCP scenarios, applying a 5% and 10% adaptation scenario would result in a lower temperature-attributable burden (Table 3). For example, with a 10% adaptation scenario, the temperature-attributable burden in 2050s would increase by 16.7% (from 35.8 YLDs to 41.8 YLDs) and 29.6% (from 35.8 YLDs to 46.4 YLDs) under RCP 4.5 and RCP 8.5, respectively (Table 4). Although the overall temperature-attributable YLDs increased in both the 2030s and 2050s under both emission scenarios, applying a 10% adaptation

Adaptation scenarios	RCP	Temperature attributable YLDs (SD) <sup>a</sup> under constant population		Temperature attributable YLDs (SD) <sup>a</sup> under Medium population growth	
		2030	2050	2030	2050
Without adaptation	4.5	41.5 (0.5) (16.5%)	45.8 (0.5) (29.3%)	55.5 (0.5) (55.0%)	76.3 (0.6) (113.4%)
	8.5	43.3 (0.5) (21.8%)	51.1 (0.6) (46.6%)	58.5 (0.5) (62.3%)	85.4 (0.6) (141.9%)
Adaptation (5%)	4.5	39.6 (0.4) (9.8%)	43.7 (0.4) (23.5%)	53.3 (0.4) (47.8%)	72.9 (0.4) (103.6%)
	8.5	41.3 (0.4) (15.9%)	48.8 (0.5) (39.9%)	55.9 (0.4) (54.5%)	81.5 (0.5) (130%)
Adaptation (10%)	4.5	37.3 (0.4) (5.3%)	41.8 (0.4) (16.7%)	50.6 (0.4) (40.5%)	69.8 (0.4) (94.1%)
	8.5	39.2 (0.4) (10.1%)	46.4 (0.5) (29.6%)	53.1 (0.4) (46.9%)	77.6 (0.4) (119.8%)

<sup>a</sup>Temperature attributable YLDs (percent change compared to the baseline period).

Table 3: Projected temperature attributable YLDs in 2030s and 2050s under scenarios of constant population and medium population growth series, two representative concentration pathways (RCP4.5, RCP8.5) and two adaptation scenarios (5% and 10% slope reduction in the ERF).

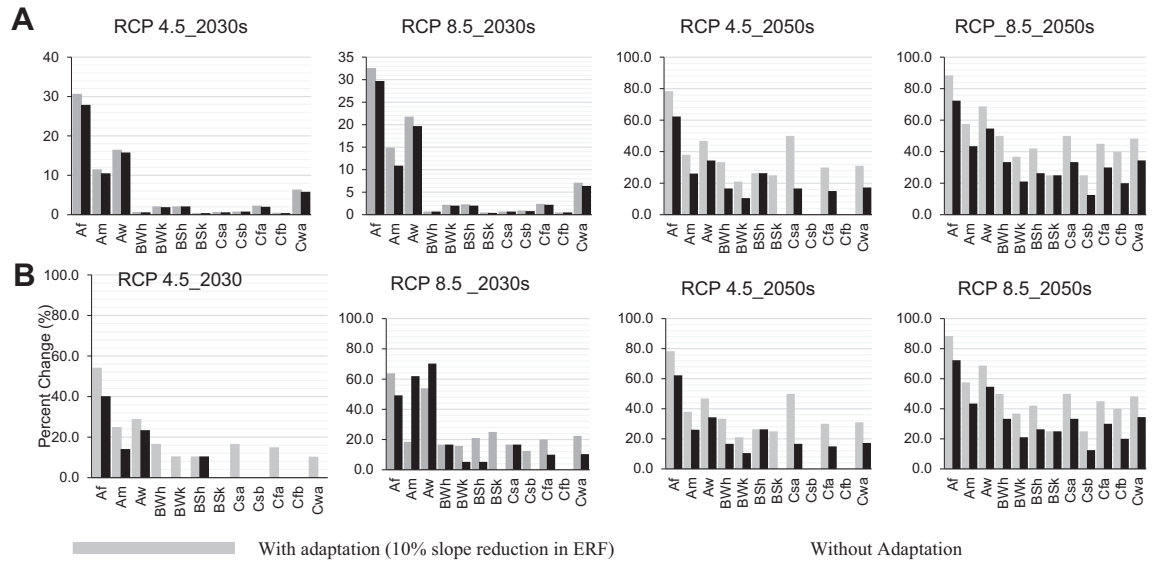


**Fig. 3:** (A) Projected YLDs per million and (B) percent changes of temperature-attributable YLDs in the 2030s and 2050s compared with the baseline period (2003–2018) under RCP 4.5 and RCP 8.5 emission scenarios in Australia.

scenario in the 2030s under RCP 4.5 reduced the temperature-attributable YLDs across most climate zones and resulted in the same YLD as the baseline period (Fig. 3 and Table S4).

A change in population size resulted in significant differences in the temperature attributable burden. For a constant population, the national temperature-attributable burden is projected to increase by 21.8% and 46.6% under RCP 8.5 in the 2030s and 2050s, respectively. In contrast under the same RCP 8.5 scenario, if the projected changes in temperature are combined with 10% adaptation scenarios and projected population growth, the temperature attributable YLDs would increase by 62.3% and 141.9% in 2030s and 2050s, respectively (Table 3).

**Sensitivity analysis**

We compared the differences in temperature attributable YLDs arising from the choice of TMRED, forms of exposure-response functions and population projection series. The results of sensitivity analyses showed variations in increasing temperature attributable YLDs due to a change in TMRED. Our findings showed that the results obtained from both average mean and median temperatures were nearly identical (Table S5). Meanwhile, MFT and 17–32 °C TMREds resulted in large difference in temperature attributable YLDs compared to the average mean annual temperature (Tables S6 and S7). In four of the 12 climate zones, change in TMRED, particularly the use of MFT resulted in a larger change in temperature attributable YLDs than a change caused by any of the other TMREds. Changing

the exposure-response function from linear to quadratic or cubic functions also resulted in a change in high temperature attributable YLDs but typically smaller than the observed variation from a change in TMRED (Table S8). Changing the population size to low and high projection series also resulted in a substantial change in temperature attributable YLDs compared to the baseline period or under the medium population projection series (Table S9). The sensitivity analyses showed a change in TMRED can lead to substantial differences in the PAF compared to altering the exposure-response function.

**Discussion**

Using YLD as an indicator, we quantified the current and future burden of RRV infection attributed to increasing mean temperature in Australia, and found that, during the baseline period, 19.1% of YLDs were attributed to increasing mean temperatures, with variations across different climate zones and jurisdictions. The Northern Territory had the highest attributable burden rate at 10.9 YLD per million population, followed by Queensland at 5.4 YLD per million. These rates were higher compared to the national average of 1.6 YLD per million. On the other hand, South Australia (excluding Tasmania and ACT with no burden) had the lowest attributable burden. Additionally, the tropical climate zones Af, Aw, and Am had higher attributable burden rates at 19.9, 12.8, and 9.2 YLD per million, respectively. The observed higher temperature attributable burden rates in the Northern Territory and



Queensland are consistent with the overall RRV burden estimated by the Australian Burden of Disease Study 2011, 2015, and 2018 studies, which showed that NT and QLD had a 50% greater burden of RRV infection compared to the national average.<sup>12</sup>

Although the relative risks per degree increase in temperature were higher than one across most climate zones, there was variation in temperature attributable YLD between jurisdictions. This was particularly noticeable in Tasmania and ACT, with nil burden related to RRV infection despite being located in climate zones with a large PAF. In contrast, only, some parts of the NT and QLD are located in tropical climate zones with the highest PAF, but showed higher burden rates at both states. The observed variation could be attributed to the complex interplay of factors such as population size, human behaviour and community health knowledge, access to health care, socioeconomic conditions, remoteness, adaptive capacities, and regional susceptibility.

We projected future temperature attributable burden of RRV under two RCP scenarios for the 2030s and 2050s, while considering two adaptation scenarios and changes in population size. The findings showed that the YLDs related to increasing mean temperature are projected to increase under both RCP emission scenarios, even with adaptation considered. The observed increase in YLDs attributable to increasing mean temperature aligns with the increase in projected temperature anomaly under RCP4.5 and RCP8.5 for 2016–2045 and 2046–2060.<sup>44</sup> However, the extent of change in temperature attributable burden showed substantial differences under different adaptation and population size changes. Without adaptation, under RCP8.5 and constant population, the temperature attributable burden is estimated to increase by 21.8% and 46.6% in 2030 and 2050, respectively.

Meanwhile, accounting with a 10% adaptation, resulted a maximum increase of 33.2% by 2050 under RCP8.5. The findings indicate that failure to consider adaptation would result in a substantial future burden associated with temperature, highlighting the need for early preventive measures.

We also found that the change in temperature attributable YLDs was greater when considering a change in population size, compared to the difference observed between RCP emission scenarios. For example, in the 2030s, the observed temperature attributable YLDs difference between RCP4.5 and RCP8.5 was only 1.8 YLDs (from 37.3 to 39.2 YLDs) under constant population and 10% adaptation. However, during the same period, under RCP 4.5 and 10% adaptation, a medium population growth resulted in an additional 13.3 YLDs (from 37.3 to 50.6 YLDs) compared to the baseline period. This highlights the significant importance of accounting for population projection when estimating the future burden of disease.<sup>45</sup> It is important to interpret the results cautiously,

as the increase correlates with a change in population size.

The results of sensitivity analyses showed significant variations in high temperature attributable burden due to alternative choices of TMRED. These findings validate the results observed in previous research, which consistently showed the importance of choosing TMREDS when calculating temperature attributable fractions for various health outcomes.<sup>46</sup> The significant variation from MFT could be due to the fact that MFT values across most climate zones including BWk, BWh, Cfa, Cfb, Csb were far below 17 °C (Table S6) which is considered the minimum temperature for transmission of RRV. It supports a preference for mean temperature over MFT based on the proximity of the mean temperature values to the minimum critical threshold (17 °C) for transmission of RRV. Considering the intricate transmission cycle of the virus and the vectors, we employed quadratic and cubic functions to explore the non-linear relationship between temperature and RRV incidence in our analysis. While differences in temperature-attributable YLDs were observed, they were minor compared to the differences observed between TMREDS.

This study had several limitations. Firstly, the absence of studies from specific climate zones necessitates relying on a single estimate to represent multiple climate zones. This becomes particularly challenging when we use a single effect estimate from one study to represent three tropical climates which could introduce a significant amount of uncertainty.

Secondly, this study focuses on the aspect of climate change specifically related to rising temperatures. However, it is important to recognize the significance of other climatic factors, particularly the impacts of altering rainfall patterns as highlighted in previous studies.<sup>7,47</sup> Further research is needed to understand the influence of climate change on rainfall patterns and its connection with RRV transmission.

Moreover, Given the complex relationship between the host, vectors and human, transmission of RRV disease by diverse mosquito species in varying climates and environmental conditions, forecasting the disease using a single set of variables will introduce further uncertainty. To fully comprehend the risks and dynamics of RRV transmission, regional climate change models must consider additional variables beyond temperature, considering the variation in RRV transmission across different regions.<sup>18</sup>

Thirdly, we assumed that the TMRED and the population growth at each SA2 level would remain constant throughout the future period. However, this assumption could potentially result in an underestimation or overestimation of the future burden. Population increases in high-risk areas, such as those adjacent to waterways or coastal marshes, may lead to a higher burden attributable to temperature than population increases in other areas.

Fourthly, due to the lack of RRs based on age and socioeconomic characteristics from the previous studies, we were not able to investigate the burden variations by age and socioeconomic groups. Moreover, when calculating the mean YLD for the baseline period, we utilized YLD data from different periods and implemented linear interpolation to fill missing data between years. This method assumes a consistent rate of change between the observed data points. However, it is crucial to acknowledge that this approach may not accurately reflect the actual underlying trend for those periods with missing data. Moreover, the limited data available for those periods made it challenging to separate the data for both calculation and validation purposes.

Lastly, our estimation of adaptation was based on empirical data, that assumed a similar slope reduction in ERF across all climate zones, which could potentially lead to an over or underestimation of future YLDs in some climate zones.

This study has several strengths. Firstly, we used YLDs related to RRV infection instead of RRV incidence. This approach allows for a direct comparison of the burden associated with RRV to other diseases for further intervention. Secondly, we investigated the attributable burden at the subnational level (states and territories) and across different climate zones, which is key to formulate effective region-specific adaptation strategies.<sup>48</sup> Thirdly, the use of daily temperature data to calculate the prevalence of exposure is another strength of this study. Daily data offers the highest temporal resolution compared to weekly or monthly data, enhancing the ability to detect short-term changes.<sup>49,50</sup> Considering the impact of temperature on various aspects of RRV transmission, the daily temperature data capture all the temporal delays in disease incidence, including the life-history, characteristics of disease vectors and hosts, contact rates, disease transmission dynamics, viral replication, and the duration between infection and the reporting of cases. Fourthly, we considered the variability in projected future increasing temperature attributable YLDs resulting from alternative TMREDS, exposure-response function, adaptation scenarios and population size. This approach enabled us to capture the uncertainty inherent in estimating the burden attributed to increasing temperature, accounting for fluctuations in the factors used in estimating future burden. Lastly, we have considered the future population size and possible adaptation scenarios. Applying both scenarios would minimize, potential overestimation or under estimation of future temperature attributable burden. This further provides public health authorities with the information needed to inform decisions, target action and develop sustainable health systems capable of meeting the challenges posed by climate change.

This study presented the current and future burden of RRV infection attributed to increasing mean temperature using YLDs as an indicator of the burden of disease. Overall, rising temperature increases the burden of RRV infection but varies across different climate zones and judications in Australia with higher burden in tropical climate zones. Moreover, the extent of change depends on the population size and adaptation scenarios considered. The change in population size and adaptation scenarios resulted a significant change in temperature attributable burden compared to a change resulted from a difference in emission scenarios.

The results clearly demonstrate that it is crucial to incorporate adaptation scenarios and population changes in future projections of the burden of disease associated with climate change. These findings provide valuable evidence to support policy decisions and guide the allocation of resources towards mitigating the future impact of RRV in the context of climate change.

#### Contributors

YTD was involved in conceptualization, study design, data curation, data analysis, data interpretation, figure creation, writing, reviewing, and revising the manuscript. BMV, OA, MT, and PB were involved in conceptualization, study design, and reviewing and revising the manuscript. AH, KD, YZ, GM, TD, TC, MG, and VP were involved in reviewing and revising the manuscript. All authors made substantial contributions to this study. YTD and BMV gathered the data, accessed the underlying data, and approved it. All authors read and approved the final version of the manuscript and agreed to submit it for publication.

#### Data sharing statement

This manuscript utilizes data collected from the Australian Institute of Health and Welfare (AIHW), which serves as the official custodian of health data in Australia. The data can be accessed online: <https://www.aihw.gov.au/reports/burden-of-disease/abds-2018-interactive-data-disease-burden/contents/state-and-territory-estimate>.

#### Editor note

The Lancet Group takes a neutral position with respect to territorial claims in published maps and institutional affiliations.

#### Declaration of interests

The authors declare that they have no known competing financial interests or personal relationships that could have appeared to influence the work reported in this paper.

#### Acknowledgements

YTD is PhD student sponsored by the University of Adelaide under the Adelaide Scholarship International scholarship scheme and this project has been funded by the Australia Research Council Discovery Program (DP200102571). We would also like to extend our gratitude to Dr. Jingwen Liu for her valuable guidance in data analysis.

#### Appendix A. Supplementary data

Supplementary data related to this article can be found at <https://doi.org/10.1016/j.lanwpc.2024.101124>.

#### References

- 1 Bellone R, Failloux A-B. The role of temperature in shaping mosquito-borne viruses transmission. *Front Microbiol.* 2020;11:584846.

- 2 Mordecai EA, Cohen JM, Evans MV, et al. Detecting the impact of temperature on transmission of Zika, dengue, and chikungunya using mechanistic models. *PLoS Neglected Trop Dis*. 2017;11(4):e0005568.
- 3 van der Wiel K, Bintanja R. Contribution of climatic changes in mean and variability to monthly temperature and precipitation extremes. *Commun Earth Environ*. 2021;2(1):1. <https://doi.org/10.1038/s43247-020-00077-4>.
- 4 Campbell-Lendrum D, Manga L, Bagayoko M, Sommerfeld J. Climate change and vector-borne diseases: what are the implications for public health research and policy? *Philos Trans R Soc Lond B Biol Sci*. 2015;370(1665). <https://doi.org/10.1098/rstb.2013.0552>.
- 5 Tong S, Dale P, Nicholls N, Mackenzie JS, Wolff R, McMichael AJ. Climate variability, social and environmental factors, and Ross river virus transmission: research development and future research needs. *Environ Health Perspect*. 2008;116(12):1591–1597. <https://doi.org/10.1289/ehp.11680>.
- 6 Caminade C, McIntyre KM, Jones AE. Impact of recent and future climate change on vector-borne diseases. *Ann N Y Acad Sci*. 2019;1436(1):157–173. <https://doi.org/10.1111/nyas.13950>.
- 7 Yu W, Dale P, Turner L, Tong S. Projecting the impact of climate change on the transmission of Ross River virus: methodological challenges and research needs. *Epidemiol Infect*. 2014;142(10):2013–2023. <https://doi.org/10.1017/S0950268814000399>.
- 8 Fouque F, Reeder JC. Impact of past and on-going changes on climate and weather on vector-borne diseases transmission: a look at the evidence. *Infect Dis Poverty*. 2019;8(1):51. <https://doi.org/10.1186/s40249-019-0565-1>.
- 9 Ryan SJ, Carlson CJ, Mordecai EA, Johnson LR. Global expansion and redistribution of Aedes-borne virus transmission risk with climate change. *PLoS Neglected Trop Dis*. 2019;13(3):e0007213. <https://doi.org/10.1371/journal.pntd.0007213>.
- 10 Rohr JR, Cohen JM. Understanding how temperature shifts could impact infectious disease. *PLoS Biol*. 2020;18(11):e3000938. <https://doi.org/10.1371/journal.pbio.3000938>.
- 11 Harley D, Sleight A, Ritchie S. Ross River virus transmission, infection, and disease: a cross-disciplinary review. *Clin Microbiol Rev*. 2001;14(4):909–932. <https://doi.org/10.1128/cmr.14.4.909-932.2001>.
- 12 Australian Institute of Health Welfare. Australian burden of disease study. <https://www.aihw.gov.au/reports-data/health-conditions-disability-deaths/burden-of-disease/overview>. Accessed December 19, 2023.
- 13 Shockett MS, Ryan SJ, Mordecai EA. Temperature explains broad patterns of Ross River virus transmission. *Elife*. 2018;7:e37762. <https://doi.org/10.7554/eLife.37762>.
- 14 Tong S, Hu W, McMichael AJ. Climate variability and Ross River virus transmission in townsville region, Australia, 1985–1996. *Trop Med Int Health*. 2004;9(2):298–304. <https://doi.org/10.1046/j.1365-3156.2003.01175.x>.
- 15 Flies EJ, Weinstein P, Anderson SJ, Koolhof I, Foufopoulos J, Williams CR. Ross river virus and the necessity of multiscale, eco-epidemiological analyses. *J Infect Dis*. 2018;217(5):807–815. <https://doi.org/10.1093/infdis/jix615>.
- 16 Yu W, Mengersen K, Dale P, et al. Epidemiologic patterns of Ross river virus disease in Queensland, Australia, 2001–2011. *Am J Trop Med Hyg*. 2014;91(1):109–118. <https://doi.org/10.4269/ajtmh.13-0455>.
- 17 Damte Y, Tong M, Varghese BM, et al. Associations between temperature and Ross river virus infection: a systematic review and meta-analysis of epidemiological evidence. *Acta Trop*. 2022;231:106454. <https://doi.org/10.1016/j.actatropica.2022.106454>.
- 18 Tong S, Bi P, Donald K, McMichael AJ. Climate variability and Ross river virus transmission. *J Epidemiol Community*. 2002;56(8):617. <https://doi.org/10.1136/jech.56.8.617>.
- 19 Liu J, Hansen A, Varghese BM, et al. Estimating the burden of disease attributable to high ambient temperature across climate zones: methodological framework with a case study. *Int J Epidemiol*. 2023;52(3):783–795. <https://doi.org/10.1093/ije/dyac229>.
- 20 Emilie C. Contribution of causal factors to disease burden: how to interpret attributable fractions. *Breathe*. 2021;17(4):210086. <https://doi.org/10.1183/20734735.0086-2021>.
- 21 Tabachnick WJ. Challenges in predicting climate and environmental effects on vector-borne disease epistemes in a changing world. *J Exp Biol*. 2010;213(6):946–954. <https://doi.org/10.1242/jeb.037564>.
- 22 Burkart KG, Brauer M, Aravkin AY, et al. Estimating the cause-specific relative risks of non-optimal temperature on daily mortality: a two-part modelling approach applied to the Global Burden of Disease Study. *Lancet*. 2021;398(10301):685–697. [https://doi.org/10.1016/S0140-6736\(21\)01700-1](https://doi.org/10.1016/S0140-6736(21)01700-1).
- 23 Arnell NW, Lowe JA, Challinor AJ, Osborn TJ. Global and regional impacts of climate change at different levels of global temperature increase. *Climatic Change*. 2019;155(3):377–391. <https://doi.org/10.1007/s10584-019-02464-z>.
- 24 Australian Government Department of Health and Aged Care. National notifiable diseases surveillance system (NNDSS) data visualisation tool. <https://www.health.gov.au/resources/apps-and-tools/national-notifiable-diseases-surveillance-system-nndss-data-visualisation-tool>. Accessed August 20, 2023.
- 25 Scientific Information for Land Owners. Australian climate data from 1889 to yesterday. <https://www.longpaddock.qld.gov.au/silo/gridded-data/>. Accessed October 12, 2023.
- 26 Heady C, Clarke J. CCiA/CSA application ready daily data interpolated across Australia from 8 selected CMIP5 GCMs. v1. CSIRO. Service Collection; 2021. <http://hdl.handle.net/102.100.100/393871?index=1>. Accessed October 12, 2023.
- 27 Australian Bureau of Statistics. Australian Bureau of statistics Jul2021-Jun2026, statistical area level 2, ABS. <https://www.abs.gov.au/statistics/standards/australian-statistical-geography-standard-asgs-edition-3/jul2021-jun2026/main-structure-and-greater-capital-city-statistical-areas/statistical-area-level-2>. Accessed February 19, 2024.
- 28 Clarke LE EJ, Jacoby HD, Pitcher H, Reilly JM, Richels R. Scenarios of greenhouse gas emissions and atmospheric concentrations; 2007. [https://digitalcommons.unl.edu/usdoepub/6/?utm\\_source=digitalcommons.unl.edu%2Fusdoepub%2F6&utm\\_medium=PDF&utm\\_campaign=PDFCoverPages](https://digitalcommons.unl.edu/usdoepub/6/?utm_source=digitalcommons.unl.edu%2Fusdoepub%2F6&utm_medium=PDF&utm_campaign=PDFCoverPages). Accessed October 12, 2023.
- 29 van Vuuren DP, Edmonds J, Kainuma M, et al. The representative concentration pathways: an overview. *Climatic Change*. 2011;109(1):5. <https://doi.org/10.1007/s10584-011-0148-z>.
- 30 Liu J, Varghese BM, Hansen A, et al. Projection of high temperature-related burden of kidney disease in Australia under different climate change, population and adaptation scenarios: population-based study. *Lancet Reg Health West Pac*. 2023;41:100916. <https://doi.org/10.1016/j.lanwpc.2023.100916>.
- 31 Fatima SH, Rothmore P, Giles LC, Bi P. Intra-urban risk assessment of occupational injuries and illnesses associated with current and projected climate: evidence from three largest Australian cities. *Environ Res*. 2023;228:115855. <https://doi.org/10.1016/j.envres.2023.115855>.
- 32 Australian Bureau of Statistics. National, state and territory population. <https://www.abs.gov.au/statistics/people/population/population-census/2021>. Accessed September 16, 2023.
- 33 Australian Bureau of Statistics. Population projections, Australia 2017 (base)-2066. <https://www.abs.gov.au/AUSSTATS/abs@.nsf/mf/3222.0>. Accessed October 17, 2023.
- 34 Werner AK, Goater S, Carver S, Robertson G, Allen GR, Weinstein P. Environmental drivers of Ross River virus in south-eastern Tasmania, Australia: towards strengthening public health interventions. *Epidemiol Infect*. 2012;140(2):359–371. <https://doi.org/10.1017/S0950268811000446>.
- 35 Koolhof IS, Bettiol S, Carver S. Fine-temporal forecasting of outbreak probability and severity: Ross river virus in Western Australia. *Epidemiol Infect*. 2017;145(14):2949–2960. <https://doi.org/10.1017/S095026881700190x>.
- 36 Cutcher Z, Williamson E, Lynch SE, Rowe S, Clothier HJ, Firestone SM. Predictive modelling of Ross River virus notifications in southeastern Australia. *Epidemiol Infect*. 2017;145(3):440–450. <https://doi.org/10.1017/S0950268816002594>.
- 37 Bi P, Hiller JE, Cameron AS, Zhang Y, Givney R. Climate variability and Ross River virus infections in Riverland, South Australia, 1992–2004. *Epidemiol Infect*. 2009;137(10):1486–1493. <https://doi.org/10.1017/S0950268809002441>.
- 38 Ezzati M, Lopez AD, Rodgers A, Vander Hoorn S, Murray CJL. Selected major risk factors and global and regional burden of disease. *Lancet*. 2002;360(9343):1347–1360. [https://doi.org/10.1016/S0140-6736\(02\)11403-6](https://doi.org/10.1016/S0140-6736(02)11403-6).
- 39 Health A, Welfare. Australian burden of disease study: impact and causes of illness and death in Australia 2018. Canberra: AIHW; 2021.
- 40 Australian Institute of Health Welfare. Australian burden of disease study: methods and supplementary material 2018. <https://www.aihw.gov.au/reports/burden-of-disease/abds-2018-interactive-data-disease-burden>; 2021. Accessed September 21, 2023.
- 41 Gosling SN, Hondula DM, Bunker A, et al. Adaptation to climate change: a comparative analysis of modeling methods for heat-related mortality. *Environ Health Perspect*. 2017;125(8):087008. <https://doi.org/10.1289/EHP634>.

- 42 Rai M, Breitner S, Wolf K, Peters A, Schneider A, Chen K. Future temperature-related mortality considering physiological and socioeconomic adaptation: a modelling framework. *Lancet Planet Health*. 2022;6(10):e784–e792. [https://doi.org/10.1016/S2542-5196\(22\)00195-4](https://doi.org/10.1016/S2542-5196(22)00195-4).
- 43 Van Rossum G, Drake Jr FL. *Python reference manual*. Amsterdam: Centrum voor Wiskunde en Informatica; 1995.
- 44 IPCC. Climate change 2013. *The physical science basis. Contribution of working group I to the fifth assessment report of the intergovernmental panel on climate change*. Cambridge, United Kingdom and New York: Cambridge University Press; 2013.
- 45 Cole R, Hajat S, Murage P, et al. The contribution of demographic changes to future heat-related health burdens under climate change scenarios. *Environ Int*. 2023;173:107836. <https://doi.org/10.1016/j.envint.2023.107836>.
- 46 Rosen L. An intuitive approach to understanding the attributable fraction of disease due to a risk factor: the case of smoking. *Int J Environ Res Publ Health*. 2013. <https://doi.org/10.3390/ijerph10072932>.
- 47 Kelly-Hope LA, Purdie DM, Kay BH. Differences in climatic factors between Ross River virus disease outbreak and nonoutbreak years. *J Med Entomol*. 2004;41(6):1116–1122. <https://doi.org/10.1603/0022-2585-41.6.1116>.
- 48 Austin SE, Ford JD, Berrang-Ford L, Biesbroek R, Ross NA. Enabling local public health adaptation to climate change. *Soc Sci Med*. 2019;220:236–244. <https://doi.org/10.1016/j.socscimed.2018.11.002>.
- 49 Parham PE, Waldock J, Christophides GK, et al. Climate, environmental and socio-economic change: weighing up the balance in vector-borne disease transmission. *Philos Trans R Soc Lond B Biol Sci*. 2015;370(1665). <https://doi.org/10.1098/rstb.2013.0551>.
- 50 Austin SE, Ford JD, Berrang-Ford L, Araos M, Parker S, Fleury MD. Public health adaptation to climate change in Canadian jurisdictions. *Int J Environ Res Publ Health*. 2015;12(1):623–651. <https://doi.org/10.3390/ijerph120100623>.